21

Multichannel and Multispectral Image Restoration Employing Fuzzy Theory and Directional Techniques

Alberto Rosales and Volodymyr Ponomaryov
National Polytechnic Institute of México
México D.F.

1. Introduction

Satellite, Radar, Medical, High Definition Television, Virtual Reality, Electron Microscopy, etc. are some of the multispectral and multichannel image processing applications that need the restoration and denoising procedures, all these applications are part of a general image processing system scheme. All these images usually are corrupted by noise due to sensors influence, during transmission of the signals, or noise produced by environmental phenomena; these types of noise can be modelled as impulse noise, Gaussian noise, multiplicative (speckle) noise, among other. As a consequence, the application of image pre-processing (denoising) efficient schemes is a principal part in any computer vision application and includes reducing image noise without degrading its quality, edge and small fine details preservation, as well as colour properties.

The main objective of present work is to expose the justified novel approaches in restoration in denoising multichannel and multispectral images that can be used in mentioned applications. There exist in literature a lot of algorithms that process two dimensional (2D) images using fuzzy and vectorial techniques (Franke et al. (2000); Russo & Ramponi (1996); Schulte & De Witte & Nachtegael et al. (2007); Shaomin & Lucke (1994); Schulte & De Witte & Kerre (2007); Nie & Barner (2006); Morillas et al. (2006); Schulte & Morillas et al. (2007); Morillas et al. (2007; 2008); Camarena et al. (2008); Morillas et al. (2008; 2005); Ma et al. (2007); Amer & Schroder (1996)). The first approach presented above works in impulsive denoising scenario in 2D colour images. This filter uses fuzzy and directional robust technics to estimate noise presence in the sample to be processed in a local manner, employing fuzzy rules, the algorithm is capable to be adapted depending of quantity of noise detected agree to fuzzy-directional values computed under these fuzzy rules.

We compare the proposed 2D framework (*FCF* – 2*D*) with recently presented 2D *INR* filter based on fuzzy logic (Schulte & Morillas et al., 2007), this algorithm detects the noise and preserves the fine details in the multichannel image. There are other 2D algorithms that are also implemented and used in this work as comparative ones: *AMNF*, *AMNF*2 (Adaptive Multichannel Filters)(Plataniotis & Androutsos et al. (1997); Plataniotis & Venetsanopoulos (2000)); *AMNIF* (Adaptive Multichannel Filter using Influence Functions) (Ponomaryov & Gallegos et al. (2005); Ponomaryov et al. (2005)); *GVDF* (Generalized Vector Directional Filter) (Trahanias & Venetsanopoulos, 1996); *CWVDF* (Centered Weighted Vector

Source: Image Processing, Book edited by: Yung-Sheng Chen,
ISBN 978-953-307-026-1, pp. 572, December 2009, INTECH, Croatia, downloaded from SCIYO.COM

Directional Filters) (Lukac et al., 2004); and finally, *VMF_FAS* (Vector Median Filter Fast Adaptive Similarity) (Smolka et al., 2003). All these techniques described in the literature demonstrate the better results among a lot of other existed.

Most of mentioned above 2D techniques present good results in details preservation and noise suppression but they employ only one frame of a video sequence and principally can not use temporal information to distinguish noise or motion present in images and suppress the noise in a more effectively way, as well as preserve the fine details and chromaticity properties. This drawback can be efficiently solved applying the three dimensional (3D) algorithms.

It is known that the principal difference between noise suppression in still images and video sequences, where information from previous and future frames may also be available, consists of finding the efficient use of several neighbour frames during processing, taking into account a possible motion between frames. In this chapter, a novel scheme to characterize the difference between pixels is proposed introducing gradients that are connected with pixel angular directions, and additionally, robust directional processing techniques presented in (Ponomaryov, 2007) (Ponomaryov & Gallegos et al., 2006). The gathering of such two methods realizes suppression of a noise, as well as preservation of fine image details on base on designed fuzzy rules and the membership degree of motion in a 3D sliding-window. Important advantage of current filtering framework consists of using only two frames (past and present) reducing the processing requirements. We also realize the adaptation of several 2D algorithms in filtering of 3D video data: *MF 3F*, *VGVDF* (Trahanias & Venetsanopoulos, 1996), *VVMF* and *VVDKNNVMF* (Ponomaryov, 2007). Additionally, we have implemented the *VKNNF*, *VATM* (Zlokolica et al., 2006), and *VAVDATM* filters (Ponomaryov, 2007).

The video denoising can be realized in two forms: during temporal processing, or in spatio-temporal processing scheme (Zlokolica et al., 2005; Zlokolica et al., 2006), where additional 3D characteristics of a video sequence (motion and noise estimation) are researched and developed.

Fuzzy Logic techniques permits to realize 3D algorithms (Saeidi et al., 2006), assigning the adapted fuzzy weights for a mean weighted filter in video sequence denoising, or via the fuzzy gradient values on base the fuzzy rules and membership functions. Another algorithm (Zlokolica et al., 2006) applied in video sequences realizes the motion estimation employing a fuzzy logic scheme based on the gradients, which exploit only pixel magnitudes, and a spatiotemporal algorithm for noise suppression.

Many difficulties are met in image processing because the data, such as, distinction among edges, fine details, movements, noise, this yields a vague and diffuse knowledge in nature. Fuzzy set theory and fuzzy logic provides powerful tools to represent and process human knowledge in form of fuzzy *IF – THEN* rules. Whether a pixel is corrupted, or discriminating, or if a fine detail is present in a scene, are the examples where fuzzy approaches can be efficiently used (Schulte & Huysmans et al., 2006).

The fuzzy-directional proposed methodologies works in a 3D environment in a video colour denoising scheme. These algorithms make use of spatio-temporal information to detect motion and noise presence to take advantage of 2D methodologies working in 3D environment. One of the methodologies is used to smooth Gaussian noise (Fuzzy Directional Adaptive Recursive Temporal Filter for Gaussian Noise *FDARTF_G*) preserving fine details, edges and chromaticity properties, where the advantage of this 3D filter is the use of only two frames of a video sequence instead of three frames used by most 3D algorithms (*MF_3F*, *VGVDF*, *VVMF*, *VVDKNNVMF*, and *VAVDATM*, etc.). Another

methodology (Fuzzy Temporal Spatial Colour Filter *FCF-3D*) operates the same way that *FDART_G* with some other ideas and modifications for impulsive denoising.
To justify the effectiveness of 3D technical proposals, the comparison with other filtering frameworks in video denoising were used (Zlokolica et al. (2006); Ponomaryov & Gallegos et al. (2006); Schulte & Huysmans et al. (2006); Schulte & Witte et al. (2006)). Reference filters: "Fuzzy Motion Recursive Spatio-Temporal Filter" (FMRSTF) (Zlokolica et al., 2006); an adaptation of FMRSTF employing only angles instead of gradients, named as "Fuzzy Vectorial Motion Recursive Spatio-Temporal Filter" (FVMRSTF); "Video Generalized Vectorial Directional Processing" (VGVDF) (Schulte & Huysmans et al., 2006), and also "Video Median M-type K-Nearest Neighbour" (VMMKNN) described in (Ponomaryov, 2007) were used as comparison in Gaussian denoising using numerous simulations and experiments.
The algorithms *MF_3F*, *VGVDF*, *VVMF*, *VVDKNNVMF*, *VKNNF*, *VATM*, and *VAVDATM* were used as comparative ones to evaluate *FCF – 3D* rendering.
Finally, multispectral image processing in different spectrum bands taken from Landsat 7, were used to evaluate the robustness of *FCF – 2D* against other filters studied.
Under various quality criteria and multiple numerical simulations, the denoising algorithms proposed demonstrate that the new framework, employing gradients and directional values, outperform analyzed methods in suppression of noise of different nature preserving important inherent characteristics of colour image and video data as well as in multispectral images. These criteria are Pick Signal to Noise Ratio (*PSNR*), Mean Absolute Error (*MAE*), and Normalized Colour Difference (*NCD*), which characterize noise suppression, edges and fine details preservation, and chromaticity properties preservation respectively.
The chapter is organized as follows: Sec. 2 presents the proposed schemes for simultaneous denoising processing of different kinds of noise: Gaussian and impulsive noises in 2D environments. Sec. 3 explains the Spatio-Temporal algorithm procedures to suppress Gaussian and impulsive noises, which employs two frames realizing the motion and noise detection. Sec. 4.1 describes the criteria to characterize the effectiveness of the approach in the image denoising, chromaticity preservation, and in reconstruction of fine details for each a frame. Sections 4.2 and 4.3 expose the experimental results in form of the objective and subjective measures presenting the effectiveness of several proposed approaches in suppression of noise and preservation of fine details and colours against other ones. A brief conclusion is drawn in Sec. 5.

2. Robust schemes applied for first frame of colour video sequences

2.1 First frame filtering

Here, the procedure consists of Histogram Calculation, Noise Estimation, and Spatial Algorithm Operations. A mean value $\bar{x}_\beta$ (β = *Red*,*Green*,*Blue* in a colour image) is found in a 3×3 sliding processing window; later, the angle deviation between two vectors: the mean value $X = \{\bar{x}_{Red}, \bar{x}_{Green}, \bar{x}_{Blue}\}$, and the central pixel of the 3×3 sample $Y = \{x_{c(Red)}, x_{c(Green)}, x_{c(Blue)}\}$, is calculated as follows: $\theta_c = A(X,Y) = arccos\frac{(X \cdot Y)}{\|X\|\|Y\|}$, in this way, θ_c is the angle deviation of the central pixel with respect to a mean value indicating the similarity between neighbouring pixels and the central one.
To obtain the histogram suggests the interval [0,1]. Because the pixel magnitudes falls within 0 to 255, the maximum angle deviation between two pixels is achieved within the

range of 0 or 1.57 radians ([0,π/2]), in this way, with the proposed interval, the angle deviations outside of [0,1] are eliminated of histogram process calculation. If $\theta_c \leq [F/255]$, the histogram is increased in "1" in "F" position, where "F" starts to increase from 0 to 255 with increasing magnitude steps of 1 for F, respectively, until it satisfies the condition, otherwise the increment is "0". Probabilities of occurrence for each value in the histogram are computed $p_j = \left(histogram_i / \sum^{255} histogram_i\right)$. After, the mean value $\mu = \sum_{j=0}^{255} j \cdot p_j$, the variance $\sigma_\beta^2 = \sum_{j=0}^{255} (j-\mu)^2 \cdot (p_j)$, and the standard deviation (SD) $\sigma'_\beta = \sqrt{\sigma_\beta^2}$, where SD is the Gaussian noise estimator proposed. This value will be used to smooth Gaussian noise for the first frame of a colour video sequence in a spatial filter.

Two processing windows: large 5×5, and centered within this, small 3×3 are employed in the procedure. Let denote as $\theta_i = A(x_i, x_c)$ the angle deviation x_i respect to x_c, where i = 0, 1, . . . , N – 1, with $i \neq c$, N = 8 (3×3 window), and c =central pixel, as it is exposed in Fig. 1. To outperform our approach let identify uniform regions that should be processed by a fast algorithm reducing computational charge: fast algorithm is a *"Mean Weighted Filtering Algorithm"*. The IF-THEN rule that applies here is based on angle deviations to filter the first frame only: IF (θ_1 AND θ_3 AND θ_4 AND $\theta_6 \geq \tau_1$) OR (θ_0 AND θ_2 AND θ_5 AND $\theta_7 \geq \tau_1$) THEN *"MeanWeighted Filtering Algorithm"*, ELSE "Spatial Algorithm Operations", where τ_1 is a threshold defined as 0.1, this value was obtained during simulations. The "AND" operation is defined as "Logical AND", the "OR" operation is "Logical OR". Values θ_0, θ_1, . . ., θ_7 are angles within the 3×3 window defined in Fig. 1b).

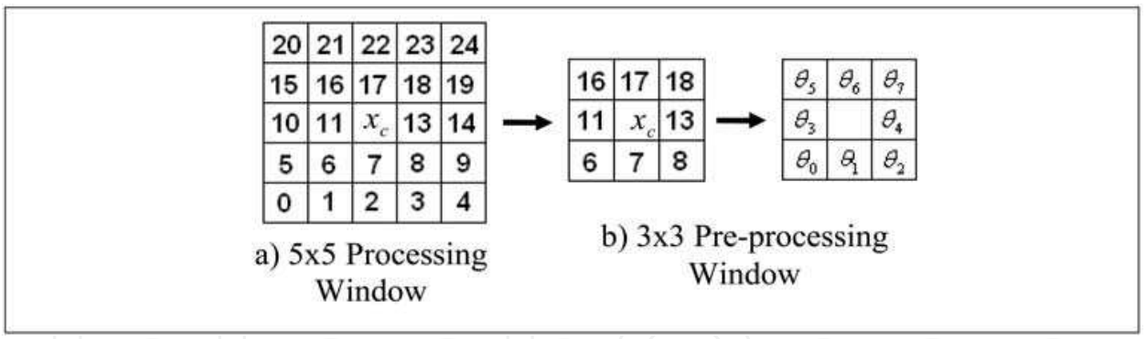

Fig. 1. Different processing windows used in First Frame Filtering.

If *"Mean Weighted Filtering Algorithm"* is selected, this algorithm makes the processing fast enough and effective in the case of noise contamination in the uniform regions, and is defined as:

$$y_{\beta out} = \left[\sum_{i=0}^{N-1} x_{\beta i} \cdot \left(\frac{2}{(1+e^{\theta_i})}\right) + x_{\beta c}\right] \Big/ \left[\sum_{i=0}^{N-1} \left(\frac{2}{(1+e^{\theta_i})}\right) + 1\right], N = 8, \text{ with } i \neq c. \quad (1)$$

Using Eq. 1 is obtained a denoised pixel component output for each channel of the first frame of a colour video.

2.2 Spatial algorithm operations

The proposed spatial processing uses the procedure in each colour plane independently obtaining values SD (σ_β) that are adapted, forming local adaptive SD. The procedure to

receive σ_β is realized using 5×5 processing window (Fig. 1a)) in the following form: $\sigma_\beta = \sqrt{\sigma_\beta^2} = \sqrt{\sum_{i=0}^{W}(x_{\beta i} - \bar{x}_{\beta 5x5})^2 \cdot (p_{\beta i})}$, and after, local adaptation is to adjust it as follows: If $\sigma_\beta < \sigma'_\beta$, then $\sigma_\beta = \sigma'_\beta$, otherwise $\sigma'_\beta < \sigma_\beta$, where σ'_β was obtained in Sec. 2.1.

Let introduce for a central pixel $x_c = x(i, j)$ of a current sample the following neighbours in the eight directions: *SW* =South-West, *S* =South, *SE* =South-East, *E* =East, *NE* =North- East, *N* = North, *NW* =North-West, and *W* =West. Fig. 2 illustrates the cardinal directions. To obtain a similarity between the central pixel and the pixels in cardinal directions for each a plane (β = *R*,*G*,*B*), let perform the following equation:

$$\nabla_{(k,l)\beta}(i,j) = |\nabla_\beta(i+k, j+l) - \nabla_\beta(i,j)|, \text{where } k,l \in \{-1,0,1\}, \tag{2}$$

These gradients are called "*basic gradient values*", and the point (*i*, *j*) is called "*the centre of the gradient values*". Two "*related (rel) gradient values*" are used, permitting to avoid blur in presence of an edge. Finally, these three gradient values for a certain direction are connected into one single general value called "*fuzzy vectorial-gradient value*" under Fuzzy Rule 1 presented later.

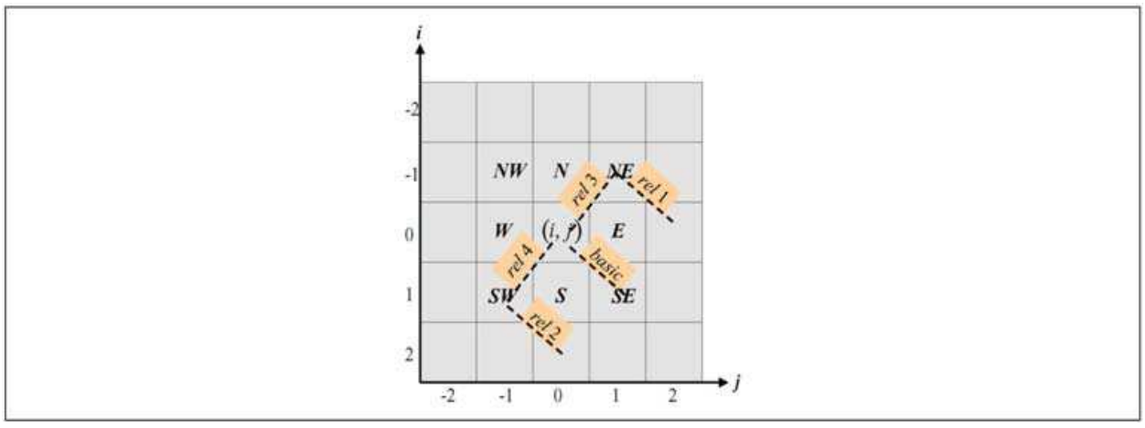

Fig. 2. Basic and related directions for gradients and angle variance (directional) values.

Now, let define γ = {*NW*,*N*,*NE*,*E*,*SE*,*S*,*SW*,*W*}, if $\nabla_{\gamma(\ell)\beta} < T_\beta$, where ℓ = {*basic*, *rel*4, *rel*3} as can be observed in Fig.2, for the "*SE*" direction only. Then, it is calculated the angle deviation in γ's directions for the basic and related magnitude component pixel values involved, where the threshold $T_\beta = 2 \cdot \sigma_\beta$ is selected according to the best performance criteria *PSNR* and *MAE*.

Let define the membership function to obtain "*Basic and Related Vectorial-Gradient Values*":

$$\mu_{NO\_NOISE} = \begin{cases} \max\{\alpha_{\gamma(\ell)\beta}, (1 - [\nabla_{\gamma(\ell)\beta}/T_\beta])\} & , \text{if} \nabla_{\gamma(\ell)\beta} < T_\beta \\ 0 & , \text{otherwise} \end{cases}, \tag{3}$$

where μ_{NO_NOISE} characterizes membership value in *NO_NOISE* fuzzy set, this set implies that basic or related component of the pixels are probably free of noise and probably belongs to an edge or fine detail, and that might be important to take them into account in

the denoising process; $\alpha_{\gamma(\ell)\beta} = \frac{2}{[1+\exp(\theta_{\gamma(\ell)\beta})]}$, and $\theta_{\gamma(\ell)\beta}$ is the angle deviation between vector pixels [255, 255, $x_{\gamma(\ell)\beta}$] and [255, 255, $x'_{\gamma(\ell)\beta}$] for each a component of a colour pixel. Finally, the process to obtain *"Fuzzy Vectorial-Gradient Values"* is defined as the Fuzzy Rule connecting Gradients with Vectorial values.

Fuzzy Rule 1: *Fuzzy Vectorial Gradient value* is defined as $\nabla_{\gamma\beta}\alpha_{\gamma\beta}$, in such a way:

IF ($\nabla_{\gamma(basic)\beta}$ IS NO NOISE AND $\nabla_{\gamma(rel4)\beta}$ is NO NOISE) OR ($\nabla_{\gamma(rel3)\beta}$ is NO NOISE AND $\nabla_{\gamma\beta D2}$ is NO NOISE) THEN $\nabla_{\gamma\beta}\alpha_{\gamma\beta}$ is NO NOISE.

The final step to filter out noise is realized using a Weighted Mean procedure with *Fuzzy Vectorial Gradient values* taken as fuzzy weights:

$$y_{\beta out} = \sum_{\gamma,\beta} (\nabla_{\gamma\beta}\alpha_{\gamma\beta}) \cdot x_{\gamma\beta} \Big/ \sum_{\gamma,\beta} (\nabla_{\gamma\beta}\alpha_{\gamma\beta}) \tag{4}$$

where $x_{\gamma\beta}$ represents each pixel within the pre-processing window used (Fig. 1b)).

2.3 Fuzzy 2D colour scheme in impulsive denoising

For impulsive noise suppression is necessary to consider not only one *"basic gradient value"* for any direction, but also four *"related gradient values"* (Fig. 2). Function , with $\Im$ ={*basic*, *rel*1, *rel*2, *rel*3, *rel*4} as illustrated in Fig. 2 for the "*SE*" direction only, where the gradient values for each a direction are shown, and parameter γ marks any chosen direction. The Fig. 2 exhibits the pixels involved in each of the directions. For example, for the "SE" direction (Fig. 2), the gradients are as follows:

Now that we have magnitude difference values, let proceed to obtain angle difference values. Let introduce the angle variance for each a channel in such a way

. For example, in the "SE" direction, the "basic" and "related" vectorial values can be written as: $\theta^{\beta}_{(1,1)}x(0,0) = \theta^{\beta}_{SE(basic)}$, $\theta^{\beta}_{(0,2)}x(i-1,j+1) = \theta^{\beta}_{SE(rel1)}$, $\theta^{\beta}_{(2,0)}x(i+1,j-1) = \theta^{\beta}_{SE(rel2)}$, $\theta^{\beta}_{(0,0)}x(i-1,j+1) = \theta^{\beta}_{SE(rel3)}$, and $\theta^{\beta}_{(0,0)}x(i+1,j-1) = \nabla^{\beta}_{SE(rel4)\gamma}$ according to Fig. 2.

Figure 2 shows the pixels used in the processing procedure for the selected cardinal direction "SE" for the basic and four related components.

Let introduce fuzzy sets, BIG and SMALL that permit estimating the noise presence in a central pixel for window 5×5 (Fig. 2). A big membership level (near to value one) in the SMALL set shows that the central pixel is free of noise, and a large membership level in the BIG set demonstrates that central pixel is highly probably noisy. The Gaussian membership functions are used to calculate membership degrees for fuzzy gradient μ_{∇} and fuzzy vectorial μ_{θ} values:

$$\mu_{\nabla^{\beta}_{\gamma(\Im)}}(SMALL,BIG) = \begin{cases} 1, & \text{if}(\nabla^{\beta}_{\gamma(\Im)} < med2, \nabla^{\beta}_{\gamma(\Im)} > med1) \\ \left(\exp\left(-\left\{\frac{(\nabla^{\beta}_{\gamma(\Im)}-med2)^2}{2\sigma_1^2}\right\}\right)\right), \left(\exp\left(-\left\{\frac{(\nabla^{\beta}_{\gamma(\Im)}-med1)^2}{2\sigma_1^2}\right\}\right)\right) & \text{, otherwise} \end{cases} \tag{5}$$

$$\mu_{\theta^{\beta}_{\gamma(\Im)}}(SMALL,BIG)=\begin{cases}1, & \text{if}(\theta^{\beta}_{\gamma(\Im)}<med4,\theta^{\beta}_{\gamma(\Im)}>med3)\\ \left(\exp\left(-\left\{\frac{(\theta^{\beta}_{\gamma(\Im)}-med4)^2}{2\sigma_2^2}\right\}\right)\right),\left(\exp\left(-\left\{\frac{(\theta^{\beta}_{\gamma(\Im)}-med3)^2}{2\sigma_2^2}\right\}\right)\right) & ,\text{otherwise}\end{cases}, \quad (6)$$

where $med1=60, med2=10, \sigma_1^2=1000, med3=0.615, med4=0.1$, and $\sigma_2^2=0.8$ were obtained according to the best PSNR and MAE criteria results.

Fuzzy Rules in 2D Filtering

Let present novel fuzzy rules applied for gradient values and vectorial values in each channel.

Fuzzy Rule A introduces the membership level of $x^{\beta}_{(i,j)}$ in the set BIG for any γ direction: IF ($\nabla^{\beta}_{\gamma\,(basic)}$ is BIG AND $\nabla^{\beta}_{\gamma\,(rel1)}$ is SMALL AND $\nabla^{\beta}_{\gamma\,(rel2)}$ is SMALL AND $\nabla^{\beta}_{\gamma\,(rel3)}$ is BIG AND $\nabla^{\beta}_{\gamma\,(rel4)}$ is BIG) AND ($\theta^{\beta}_{\gamma\,(basic)}$ is BIG AND $\theta^{\beta}_{\gamma\,(rel1)}$ is SMALL AND $\theta^{\beta}_{\gamma\,(rel2)}$ is SMALL AND $\theta^{\beta}_{\gamma\,(rel3)}$ is BIG AND $\theta^{\beta}_{\gamma\,(rel4)}$ is BIG) THEN $\nabla^{\beta F}_{\gamma}\theta^{\beta F}_{\gamma}$ *fuzzy gradient-directional value* is BIG. The operator AND outside of the parenthesis is applied as $min(A,B)$, and inside of the parenthesis is realized as A AND $B = A * B$.

Fuzzy Rule B presents the *noisy factor* (r^{β}) gathering eight *fuzzy gradient-directional values* that are calculated for each a direction as: IF *fuzzy gradient-directional values* $\nabla^{\beta F}_{N}\theta^{\beta F}_{N}$ is BIG OR $\nabla^{\beta F}_{S}\theta^{\beta F}_{S}$ is BIG OR $\nabla^{\beta F}_{E}\theta^{\beta F}_{E}$ is BIG OR $\nabla^{\beta F}_{W}\theta^{\beta F}_{W}$ is BIG OR $\nabla^{\beta F}_{SW}\theta^{\beta F}_{SW}$ is BIG OR $\nabla^{\beta F}_{NE}\theta^{\beta F}_{NE}$ is BIG OR $\nabla^{\beta F}_{NW}\theta^{\beta F}_{NW}$ is BIG OR $\nabla^{\beta F}_{SE}\theta^{\beta F}_{SE}$ is BIG THEN r^{β}(*noisy factor*) is BIG. The operation OR is introduced as $max(A,B)$.

The noisy factor is employed as a threshold to distinguish between a *noisy pixel* and a *free noise* one. So, if $r^{\beta}\geq 0.3$, the filtering procedure is applied employing the *fuzzy gradientdirectional values* as weights, in opposite case, the output is presented as unchanged central pixel: $y^{\beta}_{out}=x^{\beta}_{(i,j)}=x^{\beta}_{c}$ (Fig. 3).

For $r^{\beta}\geq 0.3$ (the value 0.3 was selected during simulations and is based on the best values for *PSNR* and *MAE* criteria), the fuzzy weights are used in the standard negator function ($\varsigma(x) = 1 - x$, $x \in [0,1]$) defined as $\zeta^{\beta F}_{\gamma}=1-\nabla^{\beta F}_{\gamma}\theta^{\beta F}_{\gamma}$, where $\nabla^{\beta F}_{\gamma}\theta^{\beta F}_{\gamma}\in[0,1]$. So, this value origins the fuzzy membership value in a new fuzzy set defined as "NO BIG" (noise free) where the fuzzy weight for central pixel in NO BIG fuzzy set is $\zeta^{\beta F}_{c=(0,0)}=3\cdot\sqrt{1-r^{\beta}}$. Scheme showed in Fig. 3 performs denoising process using fuzzy values as fuzzy weights, where $\gamma\in\dot{\gamma}$, $\dot{\gamma}$= {*NW*,*N*,*NE*,*E*,*SE*,*S*,*SW*,*W*, and *c*(central pixel)}.

So, the output's filtering result is formed by selecting one of the neighbouring pixels from the j^{th} ordered values including central component, this procedure prevents the smoothing of a frame. The condition $j \leq 2$ permits to avoid selection of the farther pixels, but if $j \leq 2$ condition is not satisfied, it should be upgraded the total weight.

3. Spatio-temporal algorithm procedures to suppress noise

3.1 3D additive noise filtering

To avoid smoothing of fine details and edges, designing a temporal algorithm for motion detection in the past and present frames (t–1 and t frames) of a colour video sequence. A better preservation of the image characteristics (edges, fine details and chromaticity preservation) was obtained applying this scheme.

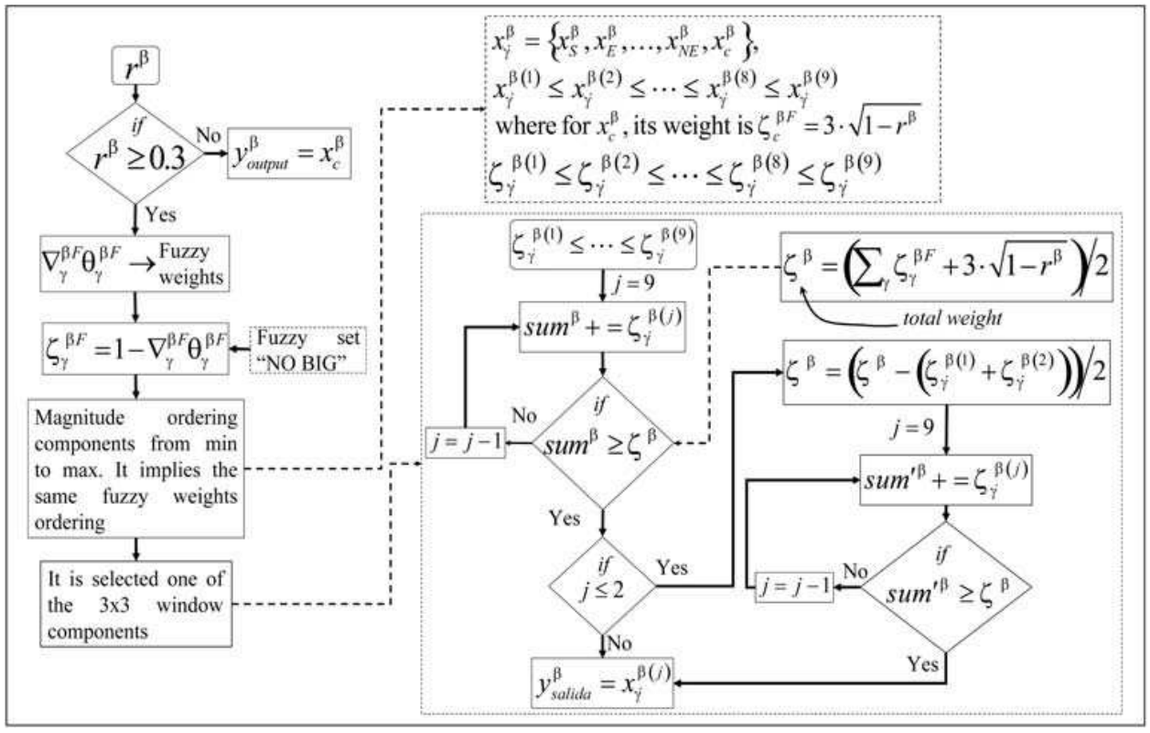

Fig. 3. Impulsive denoising scheme, using *fuzzy gradient-directional values* for the Spatial Filtering.

To characterize the similarity between two frames (*past* and *present* frames), it is necessary to obtain a relation of similarity between them. Using the gradient values and the angle deviations between pixels belonging to each frame, it is possible to compute a similarity level, which characterizes the motion and noise levels in the central sample in the present (*t*) frame.

The angle deviations and the gradient values related to a central pixel in the present frame respect to its neighbours from past frame are found accordingly to the first expression in equation 7(a):

$$\begin{aligned} &(\theta^1_{\beta i} = A(x^{t-1}_{\beta i}, x^t_{\beta c}), \nabla^1_{\beta i} = |\, x^{t-1}_{\beta i} - x^t_{\beta c}\,|), \text{ (a)} \\ &(\theta^2_{\beta i} = A(x^{t-1}_{\beta i}, x^t_{\beta i}), \nabla^2_{\beta i} = |\, x^{t-1}_{\beta i} - x^t_{\beta i}\,|), \text{ (b)} \\ &(\theta^3_{\beta i} = A(x^t_{\beta i}, x^t_{\beta c}), \nabla^3_{\beta i} = |\, x^t_{\beta i} - x^t_{\beta c}\,|), \text{ (c)}, \end{aligned} \tag{7}$$

where $i = 0, \ldots, N-1$; $N = 8$, $x^t_{\beta c}$ is a central pixel channel in the present frame, and $t-1$ and t parameters mark the past and present frames, respectively. The angle and gradient values in both frames are calculated according to equation 7(b). Finally, the same parameters for the present frame are only employed, eliminating operations in past frame as in equation 7(c). This framework is better understood following Fig. 4.

The membership functions of fuzzy sets SMALL and BIG are defined similarly to equations (5) and (6):

$$\mu_{SMALL(\chi)} = \begin{cases} 1, & \text{if } \chi < \mu_1 \\ \exp\left(-\left\{\frac{(\chi-\mu_1)^2}{2\sigma^2}\right\}\right), & \text{otherwise} \end{cases}, \tag{8}$$

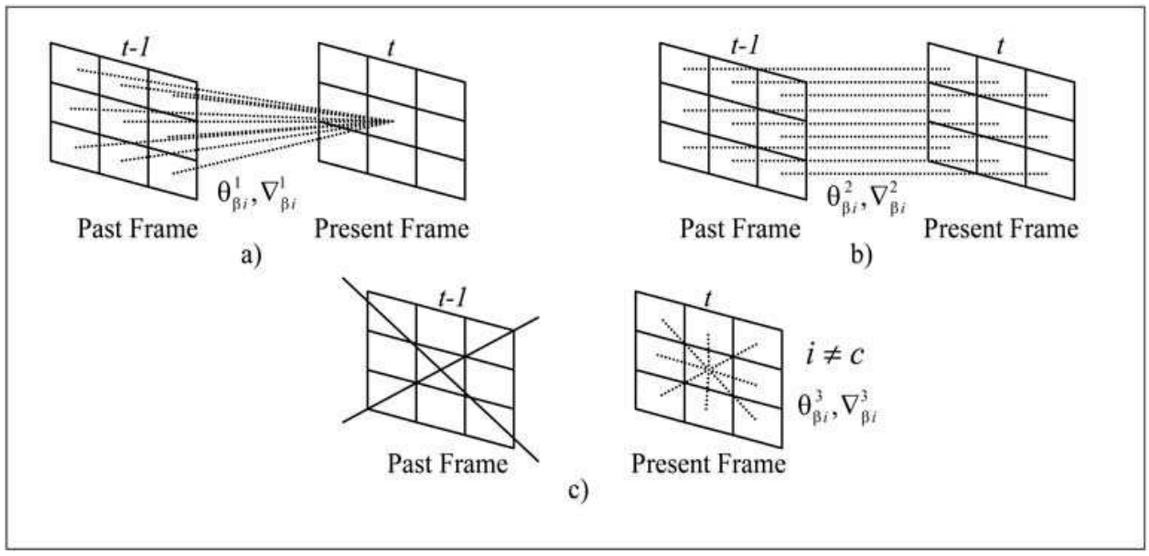

Fig. 4. Procedures used for angle and gradient values in neighbouring frames.

$$\mu_{BIG(\chi)} = \begin{cases} 1, & \text{if } \chi > \mu_2 \\ \exp\left(-\left\{\frac{(\chi-\mu_2)^2}{2\sigma^2}\right\}\right), & \text{otherwise} \end{cases}, \tag{9}$$

where $\chi = \theta, \nabla$, with respective parameters $\mu_1 = \phi_1, \phi_2$, $\mu_2 = \phi_3, \phi_4$, and $\phi_1 = 0.2$, $\phi_2 = 60$, $\phi_3 = 0.9$, $\phi_4 = 140$, using $\sigma_2 = 0.1$ for ϕ_1 and ϕ_3, and using $\sigma_2 = 1000$ for ϕ_2 and ϕ_4 respectively.

The designed fuzzy rules are used to detect the *movement presence* and/or *noise* analyzing pixel by pixel. First, detecting motion relative to the central pixel in the present frame with the pixels in the past frame (Fig. 4(a)) are found. Secondly, the movement detection in respect to pixel by pixel in both positions of the frames (Fig. 4(b)) is realized. Finally, this procedure is only applied in the present frame using central pixel and its neighbours (Fig. 4(c)). These three movement values are used to define the parameter that characterizes the *movement/noise confidence*. The fuzzy rules presented below are illustrated in Fig. 5.

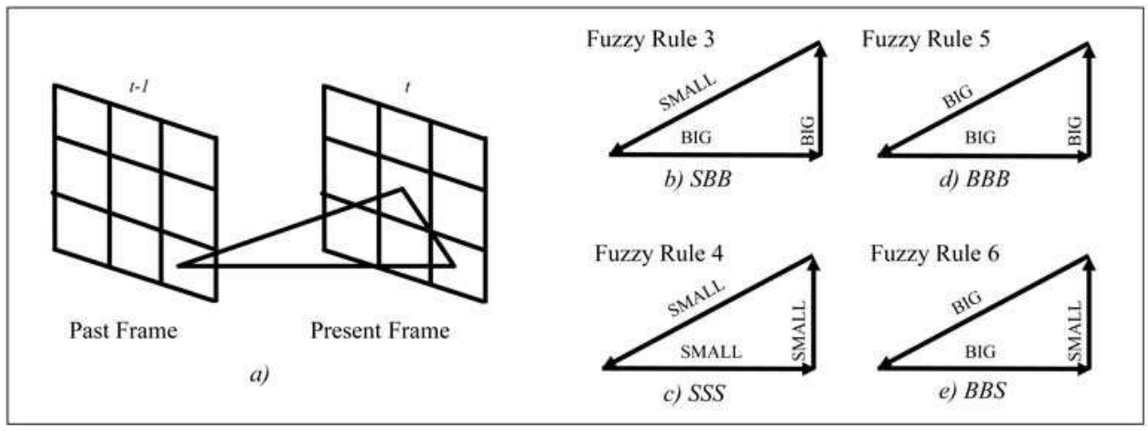

Fig. 5. **Fuzzy Rules** 3–6 in determination of the *movement/noise confidence* in past and present frames.

The following fuzzy rules were designed to detect changes in magnitude and angle deviations between the central and neighbour pixels in *t* and *t*–1 frames, this characterizes the motion and noise levels in the central pixel and its neighbourhood.

Fuzzy Rule 3: Definition of the *Fuzzy Vectorial-Gradient value* $SBB_{\beta i}$: IF $\theta^1_{\beta i}$ is SMALL AND $\theta^2_{\beta i}$ is BIG AND $\theta^3_{\beta i, i\neq c}$ is BIG AND $\nabla^1_{\beta i}$ is SMALL AND $\nabla^2_{\beta i}$ is BIG AND $\nabla^3_{\beta i, i\neq c}$ is BIG THEN $SBB_{\beta i}$ is true (Fig. 5b).

Fuzzy Rule 4: Definition of the *Fuzzy Vectorial-Gradient value* $SSS_{\beta i}$. IF $\theta^1_{\beta i}$ is SMALL AND $\theta^2_{\beta i}$ is SMALL AND $\theta^3_{\beta i, i\neq c}$ is SMALL AND $\nabla^1_{\beta i}$ is SMALL AND $\nabla^2_{\beta i}$ is SMALL AND $\nabla^3_{\beta i, i\neq c}$ is SMALL THEN $SSS_{\beta i}$ is true (Fig. 5c)).

Fuzzy Rule 5: Definition of the *Fuzzy Vectorial-Gradient value* $BBB_{\beta i}$. IF $\theta^1_{\beta i}$ is BIG AND $\theta^2_{\beta i}$ is BIG AND $\theta^3_{\beta i, i\neq c}$ is BIG AND $\nabla^1_{\beta i}$ is BIG AND $\nabla^2_{\beta i}$ is BIG AND $\nabla^3_{\beta i, i\neq c}$ is BIG THEN $SSS_{\beta i}$ is true (Fig. 5d)).

Fuzzy Rule 6: Definition of the *Fuzzy Vectorial-Gradient value* $BBS_{\beta i}$. IF $\theta^1_{\beta i}$ is BIG AND $\theta^2_{\beta i}$ is BIG AND $\theta^3_{\beta i, i\neq c}$ is SMALL AND $\nabla^1_{\beta i}$ is BIG AND $\nabla^2_{\beta i}$ is BIG AND $\nabla^3_{\beta i, i\neq c}$ is SMALL THEN $BBS_{\beta i}$ is true (Fig. 5e)).

The *SD* of the sample to a 3×3×2 pre-processing window for each a colour channel in the past and present frames is calculated obtaining the parameter σ''_β, which is described as a *Temporal SD*. Procedure to calculate σ''_β is similar to used in Sec. 2.1, but applied for the 3×3×2 samples. After that, we compare it with *SD* σ'_β obtained for Spatial Filter (Sec. 2.1) in a following way: *if* $\{(\sigma''_{red} \geq 0.4 * \sigma'_{red})$ AND $(\sigma''_{green} \geq 0.4 * \sigma'_{green})$ AND $(\sigma''_{blue} \geq 0.4 * \sigma'_{blue})\}$, *then* Fuzzy Rules 3, 4, 5, and 6 should be employed, otherwise, a *Mean Filter* must be performed. The AND operation is the "Logical AND" in presented above *if-then* condition. So, the application of the *Mean Filter Algorithm*: $\bar{y}_{\beta out} = \sum_{i=1}^{M} x_{\beta i} \Big/ M$, M = 18 signifies that a uniform area is under processing.

The updating of the *Standard Deviation "SD"* that should be used in the processing of next frame is realized according to equation: $\sigma'_\beta = (\alpha \cdot (\sigma_{total}/5)) + ((1 - \alpha) \cdot \sigma'_\beta)$, where $\sigma_{total} = (\sigma''_{red} + \sigma''_{green} + \sigma''_{blue})/3$. Sensitive parameter "$\alpha$" is chosen: for *Mean Filter Algorithm* and fuzzy value *SSS*, α = 0.125, and for fuzzy values *SSB* and *BBS*, α = 0.875.

The consequences, which are applied to each fuzzy rule, are based on different conditions that might be present in the sample: *the sample is in movement*, or *the sample is noisy one*, or it is simply *free of noise and movement*. If conditions established in the Fig. 6 are satisfied, then, are performed the equations (10), (11), (12), and "**Procedure 1**" depending on the selected case.

$$y_{\beta out} = \frac{\sum_{i=1}^{\#pixels} x^{t-1}_{\beta i} \cdot SBB_{\beta i}}{\sum_{i=1}^{\#pixels} SBB_{\beta i}}, \text{or} \tag{10}$$

$$y_{\beta out} = \frac{\sum_{i=1}^{\#pixels} 0.5(x^{t-1}_{\beta i} + x^{t}_{\beta i}) \cdot SSS_{\beta i}}{\sum_{i=1}^{\#pixels} SSS_{\beta i}}, \text{or} \tag{11}$$

$$y_{\beta out} = \frac{\sum_{i=1}^{\#pixels} x_{\beta i}^{t} \cdot (1 - BBS_{\beta i})}{\sum_{i=1}^{\#pixels} (1 - BBS_{\beta i})} \tag{12}$$

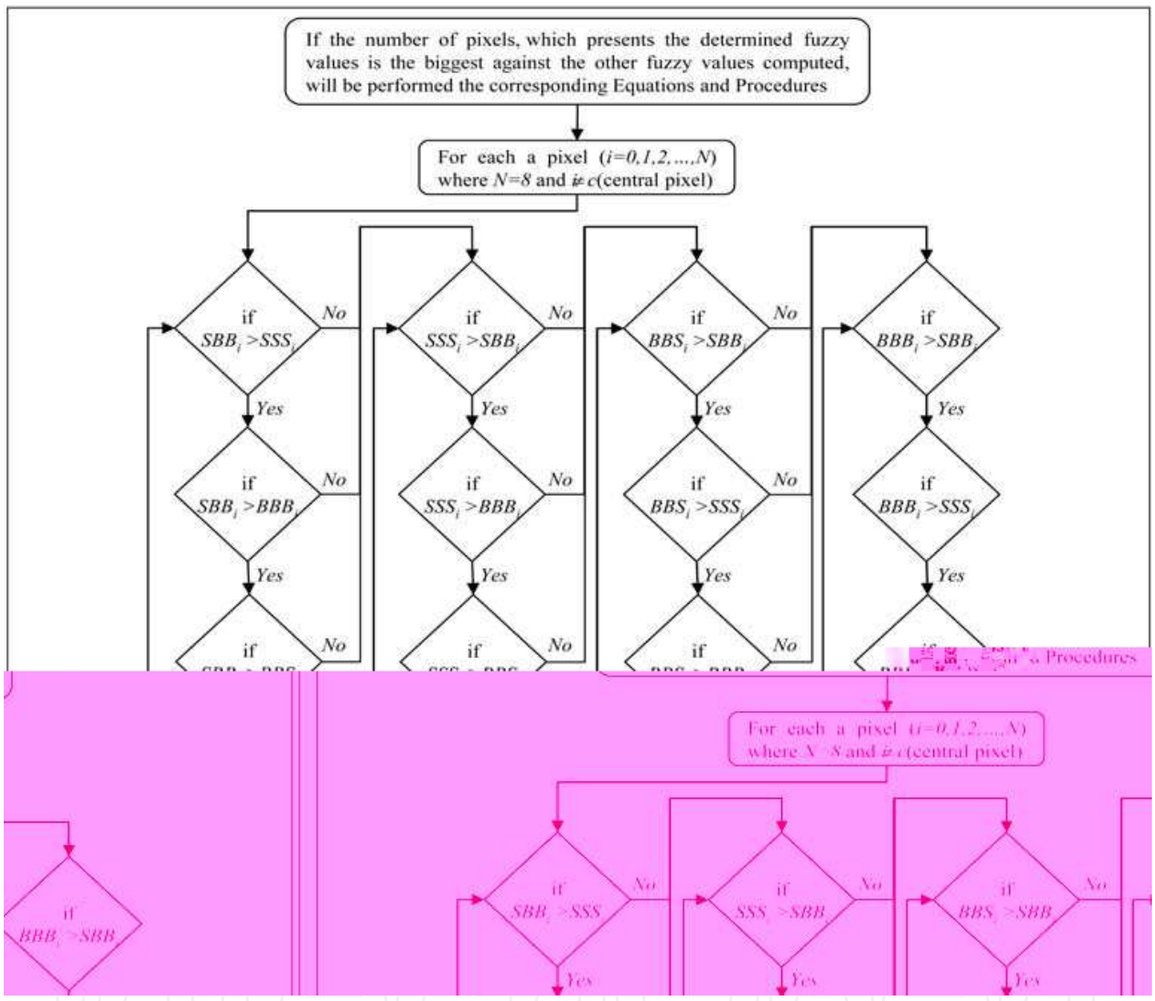

Fig. 6. Denoising scheme applied in 3D algorithm in case of *movement*, *noise*, *no movement*, *and no noise*.

Procedure 1: If the number of pixels with value $BBB_{\beta i}$ ($\#pixels_{BBB}$) is the largest reached, then consider the nine *Fuzzy Vectorial-Gradient values* obtained from *BBB*. It is selected the central value and three fuzzy neighbours values to detect motion. We conducted a combination of four subfacts, which are combined by a triangular norm defined as *A* AND *B* = *A* ∗*B*. The intersection of all possible combinations of *BBB* and three different degrees of membership BIG neighbours produces 56 values to be obtained. The values are added using an algebraic sum of all instances to obtain *the motion noise confidence*. This value is used to update the *SD* and get the output pixel using the following algorithm: $y_{\beta out} = (1-\alpha) \cdot (x_{\beta c}^{t}) + \alpha \cdot (x_{\beta c}^{t-1})$ (α=0.875, if *motion_noise confidence*= 1; α=0.125, if *motion_noise confidence* = 0, and α=0.5,

otherwise), where $x_{\beta c}^{t-1}$, and $x_{\beta c}^{t}$ represent each central pixel in the past and present frames that meets the conditions of the presented fuzzy rule.
If there is not exist the majority in pixels by any Fuzzy Rule calculated, it can be concluded that values of sample in the past and present frames have similarity nature. So, using only the central pixels from present and past frames, we can obtain an output's pixel,

$$y_{\beta out} = 0.5 \cdot x_{\beta c}^{t} + 0.5 \cdot x_{\beta c}^{t-1}, \text{ with sensitive parameter, } \alpha = 0.5. \tag{13}$$

At final step, the algorithm employs the Spatial Filter proposed in Sec. 2 for smoothing the non-stationary noise left after preceding temporal filter. This can be done by a local spatial algorithm, which adapts to the structures of the image and the noise level corresponding to the spatial neighbourhood. This algorithm needs only the modification in its threshold value: $T_\beta = 0.25\ \sigma_\beta^{'}$.

3.2 Fuzzy Colour 3D Filter (FCF-3D) for impulsive denoising

Processing two neighbour frames (past and present) of a video sequence permits to calculate the motion and noise levels of a central pixel. A 5×5×2 sliding window, which is formed by the past and present frames, is employed, and the difference values among these frames are calculated, forming a *difference magnitude frame* "λ^{β}" and a *difference directional frame* "ϕ^{β}" related with differences only, as can be seen in Fig. 7:

$$\lambda_{(k,l)}^{\beta}[x_{\beta}^{t-1}(i,j), x_{\beta}^{t}(i,j)] = \mid x_{\beta}^{t-1}(i+k, j+l) - x_{\beta}^{t}(i+k, j+l) \mid, \tag{14}$$

where $x_{\beta}^{t-1}(i,j)$ are pixels in t – 1 frame of video sequence, and $x_{\beta}^{t}(i,j)$ show the pixels in t frame, with indexes $(k, l) \in \{-2,-1, 0, 1,2\}$ (Fig.7a)).

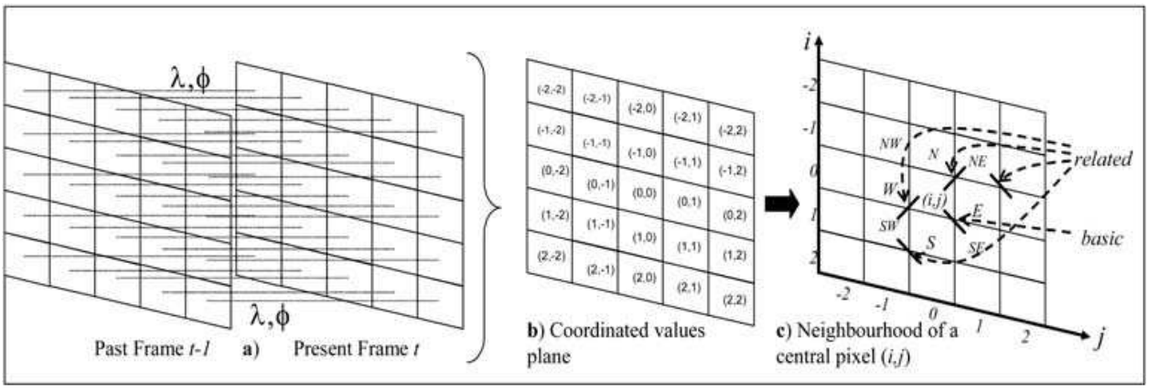

Fig. 7. a) Frames, b) Coordinated plane for *difference magnitude and directional values*, c) Neighbourhood pixels for central one.

Let calculate the absolute difference gradient values of a central pixel in respect to their neighbours for a 5*x*5*x*1 processing window (Fig. 7b) and Fig. 7c)). The *absolute difference gradient values* are calculated as in the following equation for only the *SE*(*basic*) direction:

$$\nabla_{(1,1)}^{'\beta}\lambda(0,0) = \nabla_{SE(basic)}^{'\beta}, \nabla_{SE(basic)}^{'\beta} = \mid \lambda_{(0,0)}^{\beta} - \lambda_{(1,1)}^{\beta} \mid \tag{15}$$

The same procedure should be repeated for all other basic and four related values in any direction. As in 2D framework (Sec. 2.1), calculate the *absolute difference directional values* of a central pixel with respect to its neighbours as an angle variance value among t–1 and t frames $\phi^{\beta}_{(k,l)}(x^{t-1}_{\beta}(i+k,j+l), x^{t}_{\beta}(i+k,j+l))$. Using angle variance value $\phi^{\beta}_{(k,l)}$, we can present the *absolute variance directional values* to the $SE(basic)$ direction only as:

$$\nabla''^{\beta}_{(1,1)}\phi(0,0) = \nabla''^{\beta}_{SE(basic)}, \nabla''^{\beta}_{SE(basic)} = \mid \phi^{\beta}_{(0,0)} - \phi^{\beta}_{(1,1)} \mid \tag{16}$$

The same reasoning done for $\nabla'^{\beta}_{SE(basic)}$ regarding to $\nabla^{\beta}_{SE(basic)}$ (Sec. 2.3) can also be made for $\nabla''^{\beta}_{SE(basic)}$. Let employ the same Gaussian membership functions for fuzzy values as in the equations (5) and (6), introducing the *fuzzy gradient-directional difference values*. Numerical experiments realized in this case have given the values used for the functions described in equations (5) and (6): with $med3 = 0.1$, $med4 = 0.01$ according to the best *PSNR* and *MAE* criteria results.

Fuzzy Rules in 3D Impulsive Noise Suppression

The fuzzy rules used to characterize motion and noise levels in central pixel components are defined as follows:

Fuzzy Rule 1_3D determines the **FIRST 3D fuzzy gradient-directional difference** value as $(\nabla'^{\beta F}_{\gamma}\nabla''^{\beta F}_{\gamma})_{FIRST}$: IF ($\nabla'^{\beta}_{\gamma\,(basic)}$ is BIG AND $\nabla'^{\beta}_{\gamma\,(rel1)}$ is SMALL AND $\nabla'^{\beta}_{\gamma\,(rel2)}$ is SMALL AND $\nabla'^{\beta}_{\gamma\,(rel3)}$ is BIG AND $\nabla'^{\beta}_{\gamma\,rel4)}$ is BIG) AND ($\nabla''^{\beta}_{\gamma(basic)}$ is BIG AND $\nabla''^{\beta}_{\gamma(rel1)}$ is SMALL AND $\nabla''^{\beta}_{\gamma(rel2)}$ is SMALL AND $\nabla''^{\beta}_{\gamma(rel3)}$ is BIG AND $\nabla''^{\beta}_{\gamma(rel4)}$ is BIG) THEN $(\nabla'^{\beta F}_{\gamma}\nabla''^{\beta F}_{\gamma})_{FIRST}$ is BIG. This fuzzy rule characterizes the confidence in the motion and noise in a central pixel due to neighbour fuzzy values in any γ direction. Operation "AND" outside of parenthesis is realized as $min(A,B)$.

Fuzzy Rule 2_3D defines the **SECOND 3D fuzzy gradient-directional difference** value as $(\nabla'^{\beta F}_{\gamma}\nabla'^{\beta F}_{\gamma})_{SECOND}$: IF ($\nabla\gamma(basic)'^{\beta}$ is SMALL AND $\nabla'^{\beta}_{\gamma\,(rel1)}$ is SMALL AND $\nabla'^{\beta}_{\gamma\,(rel2)}$ is SMALL) OR ($\nabla''^{\beta}_{\gamma}$is SMALL AND $\nabla''^{\beta}_{\gamma(rel1)}$ is SMALL AND $\nabla''^{\beta}_{\gamma(rel2)}$ is SMALL) THEN $(\nabla'^{\beta F}_{\gamma(basic)}\nabla''^{\beta F}_{\gamma})_{SECOND}$ is SMALL. This fuzzy rule characterizes the confidence in the no movement and no noise in a central pixel in any g direction. So, the distinctness of the different area (uniform region, edge or fine detail), where a current central pixel component belongs, can be realized using this rule. Operation "OR" is calculated as $max(A,B)$; also, "AND" inside of parenthesis is defined as $A * B$.

Fuzzy Rule 3_3D defines the **motion and noise 3D confidence factor** r^{β}: IF $((\nabla'^{\beta F}_{SE}\nabla''^{\beta F}_{SE})_{FIRST}$ is BIG OR $(\nabla'^{\beta F}_{S}\nabla''^{\beta F}_{S})_{FIRST}$ is BIG OR . . . OR $(\nabla'^{\beta F}_{N}\nabla''^{\beta F}_{N})_{FIRST}$ is BIG) THEN $r^{\beta}$is BIG. So, Fuzzy Rule 3_3D permits to calculate the *fuzzy 3D movement noisy factor* and estimate the motion and noise levels presence in a central pixel component using fuzzy values determined for all directions.

Fuzzy Rule 4_3D defines the **no movement no noise 3D confidence factor** η^{β}: IF $((\nabla'^{\beta F}_{SE}\nabla''^{\beta F}_{SE})_{SECOND}$ is SMALL OR $(\nabla'^{\beta F}_{S}\nabla''^{\beta F}_{S})_{SECOND}$ is SMALL OR . . . OR $(\nabla'^{\beta F}_{N}\nabla''^{\beta F}_{N})_{SECOND}$ is SMALL) THEN η^{β} is SMALL. The fuzzy 3D no movement-no

noisy factor allows the estimation of no movement and no noise levels presence in a central pixel component using fuzzy values determined for all directions.

The parameters r^{β} and η^{β} can be applied efficiently in a decision scheme (Fig. 8): If a central pixel component is *noisy*, or is *in movement*, or is a *free one* of both mentioned events. Fuzzy Rules from 1_3D to 4_3D determine the novel algorithm based on the fuzzy parameters.

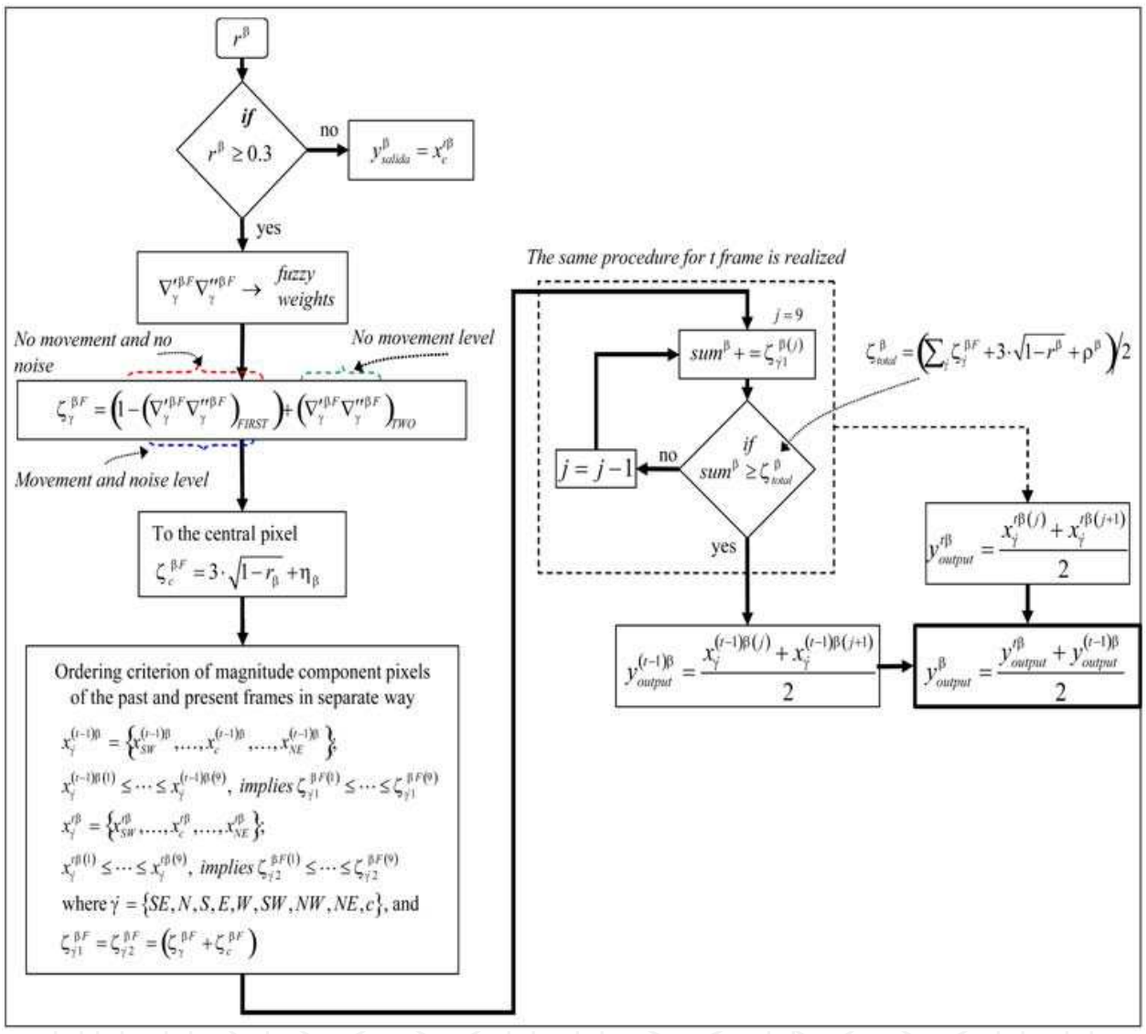

Fig. 8. Framework of the *FTSCF–3D* algorithm.

It should be chosen the *j–th* component pixel, which satisfies to the proposed conditions, ensuring that the edges and fine details will be preserved according to the selected sort ordering criterion in Fig. 8 in the selection of the nearest pixels to the central one in $t - 1$ and t frames.

Non-stationary noise that was not processed by the temporal filter, should be processed with the application of the *FCF–2D* designed in Sec. 2.3 that permits decreasing the influence of the non-stationary noise left by the temporal filter. As we are processing a frame that is free from noise, the spatial filter parameters change as follows:

- Condition $r^{\beta} \geq 0.3$ is changed to $r^{\beta} \geq 0.5$.
- The weight $\zeta^{\beta} = (\sum_{\gamma} \zeta_{\gamma}^{\beta F} + 3 \cdot \sqrt{1-r^{\beta}}) \Big/ 2$ is rearranged as follows $\zeta^{\beta} = (\sum_{\gamma} \zeta_{\gamma}^{\beta F} + 5 \cdot \sqrt{1-r^{\beta}}) \Big/ 2$.
- The central weight is modified according to $\zeta_c^{\beta F} = 5 \cdot \sqrt{1-r^{\beta}}$.
- If condition $sum^{\beta} \geq \zeta^{\beta}$ until $\zeta_{\hat{\gamma}}^{\beta F(2)}$ is not satisfied, total weight is updated according to: $\zeta^{\beta} = (\zeta^{\beta} - \zeta_{\hat{\gamma}}^{\beta F(1)}) \Big/ 2$.

4. Experimental results

4.1 Objective and subjective performances

The proposed motion-detection approach has been evaluated using different objective and subjective criteria. *PSNR* Criterion is commonly used as a measure of noise suppression:

$$PSNR = 10 \cdot \log \left[\frac{(255)^2}{MSE} \right] dB, \tag{17}$$

where the *MSE (Mean Square Error*) represents an objective measure of the square average deviation of an image estimation.
MAE criterion characterizes the edges and details preservation because it is well correlated with human visual system:

$$MAE = \frac{1}{M \cdot N} \sum_{i=0}^{M-1} \sum_{j=0}^{N-1} \left[\frac{|\, R(i,j) - R'(i,j) \,| + |\, G(i,j) - G'(i,j) \,| + |\, B(i,j) - B'(i,j) \,|}{3} \right], \tag{18}$$

The *NCD* (*Normalized Colour Difference*) measure estimates normalized perceptual error between two colour vectors in colour space $L * u * v$, and is suitable in a human perception sense. The perceptual error $\triangle E_{Luv}$ and $E_{Luv}^{*} = [(L^{*})^2 + (u^{*})^2 + (v^{*})^2]$ vector magnitude of original image pixel no corrupted are used to define *NCD*:

$$NCD = \frac{\sum_{i=0}^{M-1} \sum_{j=0}^{N-1} \| \triangle E_{Luv} \|}{\sum_{i=0}^{M-1} \sum_{j=0}^{N-1} \| E_{Luv}^{*} \|}, \tag{19}$$

where M, N is the image size, $R(i, j)$, $G(i, j)$, $B(i, j)$ are pixel values (i, j) in the plane of the original image, and $R'(i, j)$, $G'(i, j)$, $B'(i, j)$ are pixel values (i, j) for filtered image in R, G and B colour planes.
We also use a subjective visual criterion presenting the filtered images and/or their error images for implemented filters to compare the capabilities of noise suppression and detail preservation. So, a subjective visual comparison of images provides information about the spatial distortion and artifacts introduced by different filters, as well as the noise suppression quality of the algorithm and present performance of the filter, when filtering images are observed by the human visual system.

4.2 Additive noise suppression results

Different colour video sequence "*Miss America*", "*Flowers*" and "*Chair*" were used to rate the effectiveness of the proposed approach in suppression of additive noise and compare it with known techniques. They present different texture characteristics permitting a better understanding of the robustness of the proposed filtering scheme. Video sequences in the QCIF format (176×144 pixels) and in RGB colour space with 24 bits, 8 bits for each a channel were contaminated with Gaussian noise of different intensity from 0.0 to 0.05 in their SDs. The filtered frames were evaluated according to *PSNR*, *MAE*, *NCD* objective criteria, and also in subjective matter to justify the performance of the proposed filter.

The proposed Fuzzy Directional Adaptive Recursive Temporal Filtering for Gaussian noise named as *FDARTF_G* was compared with another similar one, the *FMRSTF*, which only employs the gradients. The next reference procedure, the *FVMRSTF* is some modification of *FMRSTF*, combining the gradients and angles in processing. Other two reference filters were: *VGVDF_G*, adapted to process three frames at a time, and the *VMMKNN* filter which has proven its efficiency in comparison with other filtering procedures in suppression of additive noise in grey images.

Other simulation results in Fig.9 expose the filtering performance along 43 frames of *Chair* sequence. One can clearly see that the *Chair sequence* processed by the designed procedure presents the best performance in *PSNR*, *NCD* and *MAE* criteria against other algorithms.

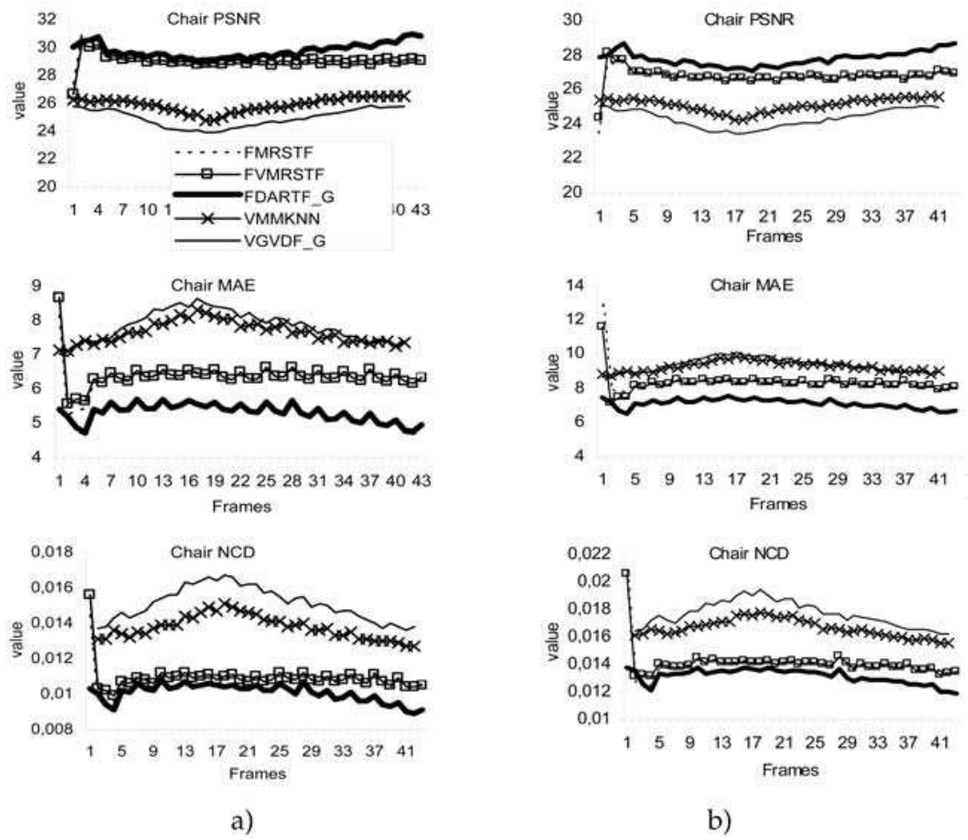

Fig. 9. *PSNR*, *MAE*, and *NCD* criteria for the first 43 frames of Chair colour sequence corrupted by noise, and processed by different algorithms. SD is equal: column a) 0.005, and column b) 0.01.

Criteria	Flowers Frame 20, Gaussian noise "SD"					Miss America Frame 20, Gaussian noise "SD"				
	FMRSTF	FVMRSTF	FDARTF_G	VMMKNN	VGVDF_G	FMRSTF	FVMRSTF	FDARTF_G	VMMKNN	VGVDF_G
SD = 0.005										
PSNR	26,192	26,007	27,309	25,348	25,46	29,926	29,905	32,51	29,799	30,658
MAE	9,628	9,825	8,503	8,777	8,959	5,818	5,826	4,459	6,178	5,549
NCD	0,016	0,017	0,015	0,015	0,017	0,02	0,02	0,016	0,021	0,02
SD = 0.01										
PSNR	24,363	24,34	25,717	24,629	24,723	27,686	27,681	30,059	27,612	28,655
MAE	11,932	11,971	10,438	9,916	10,15	7,477	7,5	6,069	8,143	7,213
NCD	0,0206	0,0208	0,0187	0,0169	0,0193	0,026	0,026	0,021	0,028	0,026
SD = 0.02										
PSNR	22,597	22,572	23,746	23,419	23.627	25,492	25,507	27,251	24,950	25,874
MAE	14,645	14,694	13,182	11,861	11.912	9,634	9,645	8,376	11,278	10,19
NCD	0,0251	0,0252	0,0234	0,0198	0,022	0,033	0,033	0,03	0,039	0,037
SD = 0.03										
PSNR	21,468	21,465	22,702	22.523	22.794	24,183	24,174	26,024	23,238	24,236
MAE	16,684	16,698	14,853	13.351	13.316	11,145	11,167	9,603	13,929	12,404
NCD	0,0285	0,0287	0,026	0,0217	0,0241	0,0384	0,0384	0,035	0,049	0,045

Table 1. Numerical results under different criteria for framework proposed and comparative ones.

Fig. 10 presents filtering results for one frame of sequence *Chair*, where the better preservation of the image details in the case of the proposed algorithm application is observed, denoting minus black dot points quantities in comparison with the second best filtering image results obtained in Fig. 10c). It is easy to see a better noise suppression observing uniform areas of the frame.

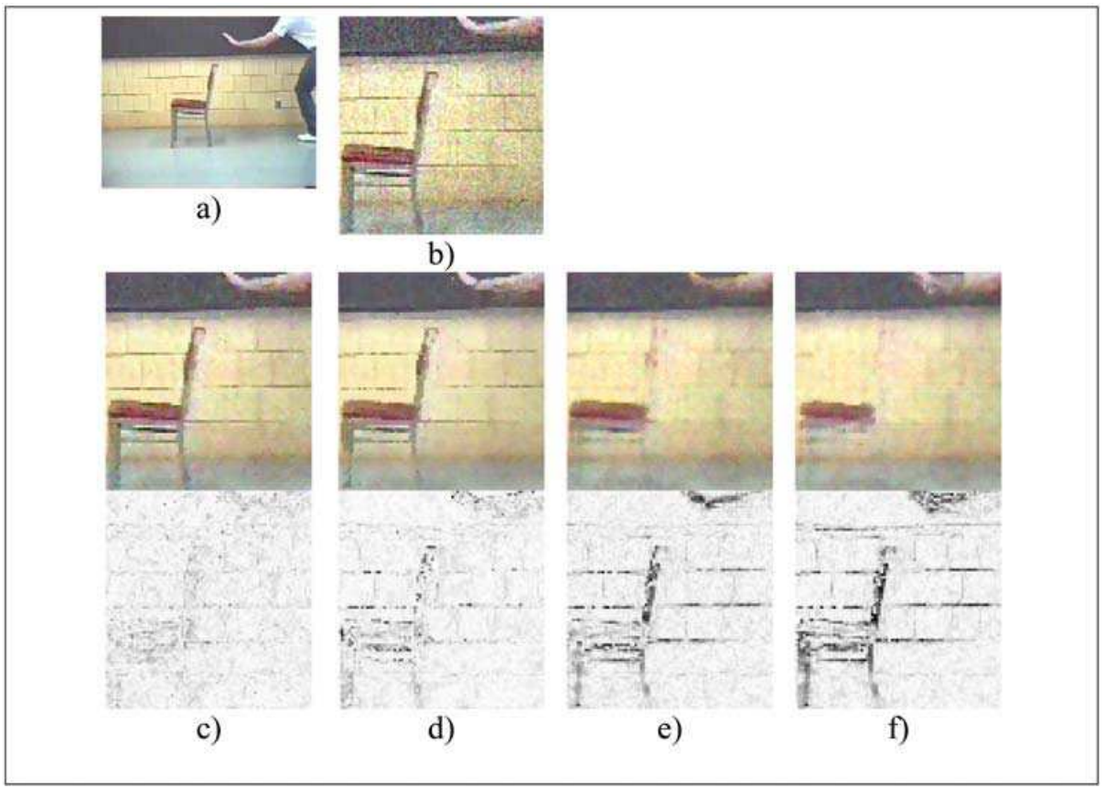

Fig. 10. Sequence Chair, frame 20; a) Original image, b) Zoomed image corrupted by Gaussian noise, *SD* = 0.005, c) *FMRSTF* filtered and error frames, d) filtered and error frames by proposed *FDARTF G*, e) *VMMKNN* filtered and error frames, f) *VGVDF G* filtered and error frames.

4.3 Impulsive noise suppression results

Test *Lena*, *Baboon*, and *Peppers* colour images and, also multichannel LandSat 7 satellite real-life images (320*x*320 pixels in RGB space, 24 bits) with different texture properties were used to evaluate 2D algorithms, as well as colour video sequence: "*Flowers*" and "*Miss America*" (QCIF format, 176*x*144 pixels in each a frame) were analyzed to characterize the performance of 3D designed filter. The frames of the video sequences were contaminated by impulsive noise with different percentages in independent way for each a channel. Table 2 presents *PSNR* and *MAE* criteria values for 2D designed algorithm against other existed ones exposing the better values in the case of low and middle noise intensity. The best performance is presented by designed scheme until 15% of noise intensity for Lena and until 10% for Baboon and Peppers colour images guaranteeing the robustness of novel framework because of different texture and chromaticity properties of the mentioned images. *MAE* criterion exposes that the best performance in preservation of the edges and fine details for mentioned images is demonstrated by designed method permitting to avoid the smoothing in wide range of noise intensity.

(%)Noise	FCF-2D	AVMF	AMNIF	CWVDF	VMF_FAS	INR
0	37,12/0,41	31,58/1;89	29,45/4,85	33,05/2,63	36,46/0,26	31,71/4,35
5	33,99/0.91	30,95/2,39	29,21/5,03	31,24/3,10	31,85/1,19	31,45/4,41
10	31,50/1,48	30,10/2,97	28,93/5,22	29,04/3,82	28,80/2,35	30,93/4,53
15	29,20/2.17	29,06/3,63	28,60/5,46	26,61/4,87	26,28/3,70	30,24/4,7
20	26,86/3.11	27,83/4,40	28,18/5,74	24,3/6,38	24,80/5,00	29,03/4,98
0	29,19/2,14	24,44/6,97	23,76/10,46	24,96/5,42	30,14/0,94	27,44/7,54
5	27,85/2.87	24,27/7,36	23,64/10,73	24,16/6,42	27,22/2,54	27,07/7,77
10	26,60/3,67	23,97/7,87	23,48/11,02	23,14/7,65	25,29/4,06	26,39/8,09
15	25,24/4,63	23,48/8,59	23,30/11,36	21,95/9,17	23,68/5,83	25,69/8,50
20	23,72/5,83	22,88/9,49	23,09/11,75	20,67/11,00	22,47/7,69	24,95/8,99
0	38,06/0,31	31,55/1,51	29,47/4,17	32,87/1,32	35,49/0,20	32,56/3,62
5	33,64/0,82	30,81/1,97	29,02/4,42	29,75/2,15	31,19/1,40	31,54/3,75
10	31,09/1,38	29,80/2,49	28,71/4,66	27,34/3,20	29,01/2,07	30,81/3,90
15	28,36/2,16	28,66/3,13	28,32/4,92	24,46/4,82	25,63/3,70	29,38/4,18
20	26,07/3,13	27,30/3,92	27,82/5,26	22,12/6,92	24,45/4,84	28,41/4,47

Table 2. *PSNR*/*MAE* criteria values for Lena, Baboon, and Peppers Images, respectively.

Multispectral image formed by 3, 2, and 1 Bands						
(%)Impulsive Noise	GVDF		MMKNN		FCF-2D	
	MAE	PSNR	MAE	PSNR	MAE	PSNR
5	13,62	21,06	13,12	22,09	4,79	25,20
15	15,44	20,17	14,49	21,33	6,97	22,99
20	16,55	19,60	15,31	20,86	8,38	21,77
25	18,05	18,85	16,31	20,33	10,24	20,44
30	19,86	18,07	17,45	19,75	12,3	19,25
Multispectral image formed by 4, 3, and 2 Bands						
5	11,92	21,75	11,40	22,94	3,77	26,2
15	13,62	20,80	12,71	22,13	5,87	23,71
20	14,678	20,20	13,54	21,57	7,28	22,33
25	16,01	19,45	14,55	20,95	9,08	20,89
30	17,58	18,68	15,70	20,29	11,16	19,55
Multispectral image formed by 4, 5, and 3 Bands						
5	11,49	21,74	10,9	23,14	3,32	26,67
15	13,11	20,84	12,19	22,3	5,46	23,96
20	14,11	20,25	13,03	21,72	6,879	22,45
25	15,30	19,60	14,03	21,06	8,65	21,00
30	16,81	18,83	15,15	20,42	10,74	19,63

Table 3. *PSNR* and *MAE* measures for different algorithms applied in the Multispectral Images.

Table 3 exposes the multispectral filtering for real life images of the same scene received from the LandSat 7 satellite in seven different bands. Objective criteria *PSNR* and *MAE* were calculated using false colour in 321, 432 and 453 bands. Filtered multispectral images can be seen in Fig. 11 for the 432 Band.

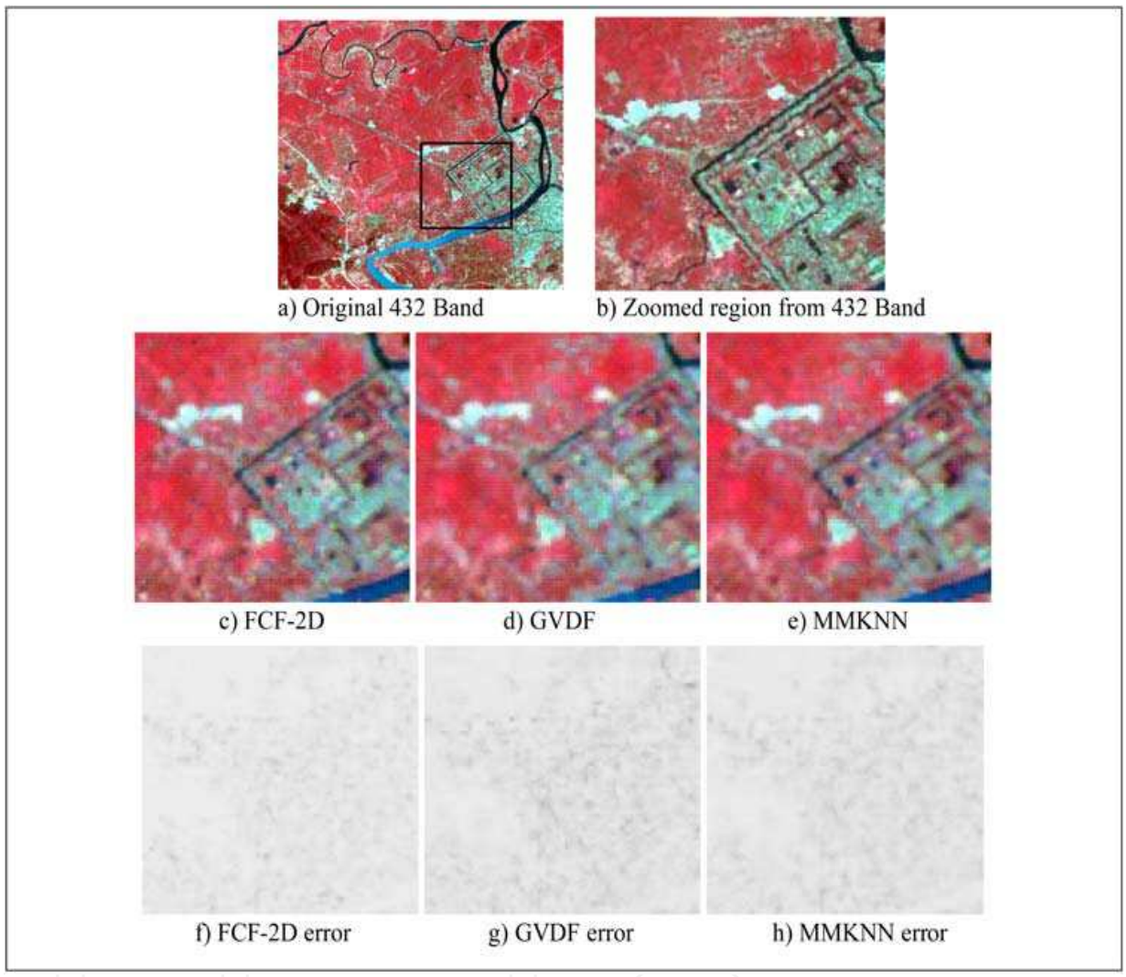

Fig. 11. Filtering and error image results in the 432 Band in a multispectral image.

In Table 4, one can see that the best performance is realized by novel 3D algorithm according to *MAE* criterion in wide range of noise contaminations, in opposite, in *PSNR* criterion values, the best performances for novel framework are found for middle, and in some cases, for high noise intensity. *NCD* criterion values exposed in the Table 5 characterize the best preservation in the chromaticity properties in wide range of noise corruption in Flowers video sequence realized by novel 3D filtering scheme confirming its robustness. Similar numerical results in less detailed video sequences, such as Miss America show that the designed algorithm demonstrates the best filtering performance in *NCD* values in wide range of noise corruption.

Subjective perception by human viewer can be observed in Fig. 12, showing in the zoomed filtered Flowers frame the better performance of the designed 3D framework in comparison with known methods, where it is clearly seen that novel algorithm preserves better the edges, fine details, and chromaticity properties against other filters.

(%)Noise	FCF-3D		MF_3F		VVMF		VVDKNNVMF		VGVDF		VAVDATM		VATM		KNNF	
	MAE	PSNR	MAE	PSNR	MAE	PSNR	MAE	PSNR	MAE	PSNR	MAE	PSNR	MAE	PSNR	MAE	PSNR
0	1,58	30,5	6,44	27,0	6,47	27.0	7,02	26,2	7,35	25,6	5,07	27,5	6,62	27,1	3,20	33,13
10	2,73	28,6	6,90	26,5	6,86	26,5	7,83	25,5	7,55	25,5	5,84	26,9	7,05	26,6	5,16	28,95
15	3,38	27,8	7,19	26,2	7,14	26,2	8,20	25,1	7,72	25,3	6,28	26,6	7,35	26,3	6,79	26,63
20	4,11	26,9	7,55	25,8	7,49	25,8	8,70	24,6	8,12	24,8	6,77	26,1	7,72	25,9	8,93	24,49
30	6,08	25,0	8,59	24,8	8,50	24,7	10,0	23,2	9,74	23,2	8,13	25,0	8,88	24,8	14,6	20,86

Table 4. *PNSR* and *MAE* criteria results for Flowers colour video sequence averaged per 100 frames.

(%)Noise	FCF-3D	MF_3F	VVMF	VVDKNNVMF	VGVDF	VAVDATM	VATM	KNNF
0	0,003	0,014	0,014	0,015	0,016	0,011	0,014	0,006
10	0,006	0,015	0,015	0,017	0,016	0,012	0,015	0,010
15	0,007	0,015	0,015	0,017	0,016	0,013	0,015	0,013
20	0,009	0,016	0,016	0,018	0,017	0,014	0,016	0,017
25	0,010	0,017	0,017	0,019	0,018	0,015	0,017	0,022
30	0,012	0,018	0,018	0,020	0,020	0,017	0,018	0,027

Table 5. *NCD* averaged values for Flowers colour video sequence.

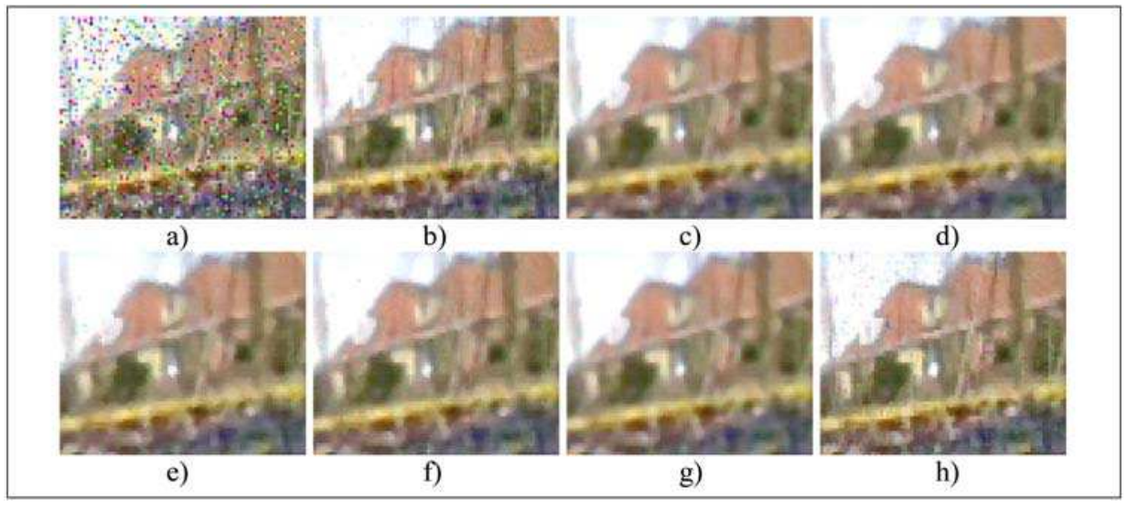

Fig. 12. a) Zoomed image region of 10*th* Flowers frame contaminated by impulsive noise of 15% intensity, b) Designed *FCF*–3*D*, c) *MF* 3*F*, d) *VVMF*, e) *VGVDF*, f) *VAVDATM*, g) *VATM*, h) *KNNF*.

Real-Time analysis was realized on the *DSP* (*TMS*320*DM*642, Texas Instruments) and is based on Reference Framework defined as *RF*5 (Mullanix & Magdic et al., 2003). Table 6 presents the processing times in some 2D and 3D algorithms, which have been implemented on *DSP*, demonstrating reliability of the proposed approach against better algorithms found in literature.

5. Conclusions

It has designed a novel structure of robust framework to remove impulse noise and additive noise in images and multichannel video sequences. Unlike existed techniques, the designed approach employs fuzzy and directional techniques to estimate motion and noise in the past and present frames showing good results. The designed fuzzy rules characterize the presence of motion and noise between the pixels in two frames (past and present frames). It has been demonstrated that the combined use of gradients and vectors improves the performance of the algorithm in comparison with cases where it is used any of this characteristics. The excellent performance of the new filtering scheme has been tested

Algorithm	Number of frames	Total Time	Max Time per frame (s)	Average Time (s)
2D Algorithms				
MF	20	0.062	0.0037	0.0031
VMF	20	0.552	0.0283	0.0278
VMF_FAS	20	41.116	2.093	2.055
AVMF	20	1.591	0.0805	0.0796
GVDF	20	117.382	5.887	5.869
CWVDF	20	58.18	5.806	2.909
FCF-2D	20	24.822	1.243	1.241
3D Algorithms				
MF_3F	20	0.114	0.0065	0.0057
VVMF	20	1.496	0.075	0.075
VATM	20	2.681	0.1347	0.134
KNNF	20	2.04	0.103	0.102
VGVDF	20	512.02	28.52	25.6
VAVDATM	20	497.356	25.551	24.867
FCF-3D	20	148.806	7.533	7.440

Table 6. 2D and 3D time processing on *DSP TMS*320*DM*642.

during numerous simulations in terms of objective criteria, as well as the subjective visual perception where the filtered images are seen by human visual system.

6. References

Amer, A. & Schroder, H. (1996). A new video noise reduction algorithm using spatial subbands, *ICECS*, vol. 1, 1996, pp. 45-48.

Camarena, G., Gregori, J., Morillas, V., & Sapena, S. (2008). Fast Detection and Removal of Impulsive Noise Using Peer Groups and Fuzzy Metrics, *Journal of Visual Communication and Image Representation*, Vol. 19, No. 1, 2008, pp. 20-29.

Franke, K., Kppen, M. & Nickolay, B. (2000). Fuzzy Image Processing by using Dubois and Prade Fuzzy Norms, *Proceedings Pattern Recognition*, Vol. 3, 2000, pp. 514-517.

Lukac, R., Smolka, B., N. Plataniotis, K. & N. Venetsanopoulos, A. (2004) Selection Weighted Vector Directional Filters, *Comput. Vision and Image Understanding*, Vol. 94, 2004, pp. 140-167.

Ma, Z. H., Wu, H. R. & Feng, D. (2007). Fuzzy vector partition filtering technique for color image restoration, *Computer Vision and Image Un-derstanding*, Vol. 107, No. 1-2, 2007, pp. 26-37.

Morillas, S., Gregori, V. & Peris-Fajarnes, G. (2008). Isolating Impulsive Noise Pixels in Color Images by Peer Group techniques, *Computer Vision and Image Understanding*, Vol.110, No. 1, 2008, pp. 102-116.

Morillas, S., Gregori, V., Peris-Fajarns, G. & Latorre, P. (2005). A fast impulsive noise color image filter using fuzzy metrics, *Real-Time Imaging*, Vol. 11, 2005, pp. 417-428.

Morillas, S., Gregori, V., Peris-Fajarnes, G. & Sapena, A. (2007). New Adaptive Vector Filter Using Fuzzy Metrics, *Journal of Electronic Imaging*, Vol. 16, No. 3, 2007, pp. 033007.

Morillas, S., Gregori, V., Peris-Fajarnes, G. & Sapena, A. (2008). Local self-adaptive fuzzy filter for impulsive noise removal in color images, *Signal Processing*, Vol. 88, No. 2, 2008, pp. 390-398.

Morillas, S., Gregori, V. & Sapena, A. (2006). Fuzzy bilateral filtering for color images, *Lecture Notes in Computer Science*, Vol. 4141, 2006, pp. 138-145.

Mullanix, T., Magdic, D., Wan, V., Lee, B., Cruickshank, B., Campbell, A., DeGraw, Y. (2003). Reference Frameworks for eXpressDSP Software: RF5, An Extensive, High Density System (SPRA795A), *Texas Instruments*, 2003.

Nie, Y. & E. Barner, K. (2006). Fuzzy Rank LUM Filters, *IEEE Trans. on Image Processing*, Vol. 15, No. 12, 2006, pp. 3636-3654.

Plataniotis, K. N., Androutsos, D., Vinayagamoorthy, S. & Venetsanopoulos, A. N. (1997). Color Image Processing Using Adaptive Multichannel Filters, *IEEE Transactions on Image Processing*, Vol. 6, No. 7, 1997, pp. 933-949.

Plataniotis, K. N. & Venetsanopoulos, A. N. (2000). *Color Image Processing and Applications*, Springer Verlag, Berlin.

Ponomaryov, V. I. (2007). Real-time 2D-3D filtering using order statistics based algorithms, *Journal of Real-Time Image Processing*, Vol. 1, No. 3, 2007, pp.173-194.

Ponomaryov, V., Gallegos-Funes, F. & Rosales-Silva, A. (2005). Real-Time Color Image Processing Using Order Statistics Filters, *Journal of Mathematical Imaging and Vision Springer*, Vol. 23, No. 3, 2005, pp. 315-319.

Ponomaryov, VI., Gallegos-Funes, FJ. &Rosales-Silva, A. (2005). Real-time color imaging based on RM-filters for impulsive noise reduction, *Journal of Imaging Science and Technology*, Vol. 49, No. 3, 2005, pp. 205-219.

Ponomaryov, V., Gallegos-Funes, F., Rosales-Silva, A. & Loboda, I. (2006). 3D vector directional filters to process video sequences, *Lecture Notes in Computer Science*, 2006, Vol. 4225, pp. 474-480.

Russo, F & Ramponi, G. (1996). A Fuzzy Filter for Images Corrupted by Impulse Noise, *Signal Processing Letters*, Vol. 3, No. 6, 1996, pp. 168-170.

Saeidi, M., Saeidi, B., Saeidi, Z. & Saeidi, K. (2006). A New Fuzzy Algorithm in Image Sequences Filtering, *Circuits, Signals, and Systems*, 2006, pp. 531-105.

Schulte, S., De Witte, V., Nachtegael, M., V. der Weken, D. & E. Kerre, E. (2006). Fuzzy Two-Step Filter for Impulse Noise Reduction From Color Images, *IEEE Trans. on Image Processing*, Vol. 15, No. 11, 2006, pp. 3567-3578.

Schulte, S., De Witte, V., Nachtegael, M., Van Der Weken D. & E. Kerre, E. (2007). Fuzzy Random Impulse Noise Reduction Method, *Fuzzy Sets and Systems*, Vol. 158, No. 3, 2007, pp. 270-283.

Schulte, S., De Witte, V. & E. Kerre, E. (2007). A Fuzzy Noise Reduction Method for Color Images, *IEEE Trans. on Image Processing*, Vol. 16, No. 5, 2007, pp. 1425-1436.

Schulte, S., Huysmans, B., Pizurica, A., E. Kerre, E. & Philips, W. (2006). A new fuzzy-based wavelet shrinkage image denoising technique, *Lecture notes Comput. Sci.*, Vol. 4179, 2006, pp. 12-23.

Schulte, S., Morillas, S., Gregori, V. & E. Kerre, E. (2007). A New Fuzzy Color Correlated Impulse Noise Reduction Method, *IEEE Trans. on Image Proc.*, Vol. 16, No. 10, 2007, pp. 2565-2575.

Shaomin, P. & Lucke, L. (1994). Fuzzy filtering for mixed noise removal during image processing, *IEEE Fuzzy Systems*, Vol. 1, 1994, pp. 89-93.

Smolka, B., Lukac, R., Chydzinski, A., N. Plataniotis, K. & Wojciechowski, W. (2003). Fast Adaptive Similarity Based Impulsive Noise Reduction Filter, *Real-Time Imaging*, Vol. 9, No. 4, 2003, pp. 261-276.

Trahanias, P. E., Venetsanopoulos, A. N. (1996). Direccional Processing of Color Images: Theory and Experimental Results, *IEEE Transactions on Image Processing*, Vo. 5, No. 6, 1996, pp. 868-880.

Zlokolica, V., De Geyter, M., Schulte, S., Pizurica, A., Philips, W. & Kerre, E. (2005). Fuzzy Logic Recursive Motion Detection for Tracking and Denoising of Video Sequences, *IS&T/SPIE Symposium on Electronic Imaging, Video Communications and Processing 5685*, 2005, pp. 771-782.

Zlokolica, V., Schulte, S., Pizurica, A., Philips, W. & Kerre (2006). Fuzzy Logic Recursive Motion Detection and denoising of Video Sequences, *Journal of Electronic Imaging*, Vol. 15, No. 2, 2006, pp. 023008.

Image Processing

Edited by Yung-Sheng Chen

ISBN 978-953-307-026-1

Hard cover, 516 pages

Publisher InTech

Published online 01, December, 2009

Published in print edition December, 2009

There are six sections in this book. The first section presents basic image processing techniques, such as image acquisition, storage, retrieval, transformation, filtering, and parallel computing. Then, some applications, such as road sign recognition, air quality monitoring, remote sensed image analysis, and diagnosis of industrial parts are considered. Subsequently, the application of image processing for the special eye examination and a newly three-dimensional digital camera are introduced. On the other hand, the section of medical imaging will show the applications of nuclear imaging, ultrasound imaging, and biology. The section of neural fuzzy presents the topics of image recognition, self-learning, image restoration, as well as evolutionary. The final section will show how to implement the hardware design based on the SoC or FPGA to accelerate image processing.

InTech Europe

University Campus STeP Ri
Slavka Krautzeka 83/A
51000 Rijeka, Croatia
Phone: +385 (51) 770 447
Fax: +385 (51) 686 166
www.intechopen.com

InTech China

Unit 405, Office Block, Hotel Equatorial Shanghai
No.65, Yan An Road (West), Shanghai, 200040, China
中国上海市延安西路65号上海国际贵都大饭店办公楼405单元
Phone: +86-21-62489820
Fax: +86-21-62489821

IntechOpen